

Alma Mater Studiorum Università di Bologna  
Archivio istituzionale della ricerca

Study of the azo-hydrazone tautomerism of Acid Orange 20 by spectroscopic techniques: UV-Visible, Raman, and surface-enhanced Raman scattering

This is the final peer-reviewed author's accepted manuscript (postprint) of the following publication:

*Published Version:*

Vannucci G., Canamares M.V., Prati S., Sanchez-Cortes S. (2020). Study of the azo-hydrazone tautomerism of Acid Orange 20 by spectroscopic techniques: UV-Visible, Raman, and surface-enhanced Raman scattering. JOURNAL OF RAMAN SPECTROSCOPY, 51(8), 1295-1304 [10.1002/jrs.5906].

*Availability:*

This version is available at: <https://hdl.handle.net/11585/789451> since: 2021-01-18

*Published:*

DOI: <http://doi.org/10.1002/jrs.5906>

*Terms of use:*

Some rights reserved. The terms and conditions for the reuse of this version of the manuscript are specified in the publishing policy. For all terms of use and more information see the publisher's website.

This item was downloaded from IRIS Università di Bologna (<https://cris.unibo.it/>).  
When citing, please refer to the published version.

(Article begins on next page)

This is the final peer-reviewed accepted manuscript of:

G. Vannucci, M.V. Cañamares, S. Prati, S. Sanchez-Cortes, Study of the azo-hydrazone tautomerism of Acid Orange 20 by spectroscopic techniques: UV–Visible, Raman, and surface-enhanced Raman scattering, *J Raman Spectrosc.* 2020; 51:1295–1304.

The final published version is available online at: <https://doi.org/10.1002/jrs.5906>

#### Terms of use:

© [2020]. This manuscript version is made available under the Creative Common Attribution-NonCommercial –NoDerivatives (CC BY-NC-ND) 4.0 International Licence.  
(<https://creativecommons.org/licenses/by-nc-nd/4.0/>)

# Study of the azo-hydrazone tautomerism of Acid Orange 20 by spectroscopic techniques: UV-Visible, Raman, and surface-enhanced Raman scattering

## Abstract

Acid Orange 20 is a synthetic monoazo dye, whose molecular structure consists of a naphthol unit and a sulfonated benzene ring linked together by an azo chromophore group. As a phenylazonaphthol with the OH group in *para* position respect to the azo group, it undergoes an azo-hydrazone tautomerism. In this work, the study of the preponderance of one tautomer over the other in different pH conditions was carried out by means of UV-Vis, Raman, and surface-enhanced Raman scattering (SERS) spectroscopies. Raman spectra of powder and aqueous solutions of the dye were obtained at different excitation lines at the natural pH of the AO20 solutions. The best results were obtained at 633 nm, and the observed Raman bands suggested the presence of the hydrazone tautomer. The molecular structure and the theoretical Raman spectra of the two tautomers were calculated by density functional theory (DFT) methods. The obtained results were used for the assignment of the Acid Orange 20 vibrational modes. The SERS analysis of the dye solutions were carried out employing Ag nanostars, pH below and above 4.7, and excitation at 442, 532, and 633 nm. The hydrazone tautomer was prevalent in most conditions. The azo tautomer was only detected at pH  $\sim$  5 under excitation with the 532 nm wavelength due to resonant Raman conditions. Finally, the effect of pH on the morphology of metal nanoparticles employed as SERS substrates was evaluated by TEM.

ARTICLE IN PRESS

Journal of Molecular Liquids, 2023, Vol. 361, Pages 118111

## 1 INTRODUCTION

The study of dyes and organic coloring materials used in artworks and cultural heritage related objects provides useful information for dating, authentication, conservation treatments, and art history in general. The number of studies and publications related to natural dyes

definitively surpasses that of synthetic ones, because the former are typically considered of more artistic and historic relevance. The conservation of modern and contemporary art is widely recognized as one of the most difficult and pressing challenges in the field. Indeed, the ease in production and employment of these new materials was responsible for their huge widespread,

accompanied by a lack of scientific knowledge and comprehension of adequate conservation treatments.<sup>[1]</sup>

Raman spectroscopy is nowadays considered an efficient non-destructive, and even *in situ*, technique for identification of inorganic pigments and other materials in artworks.<sup>[2–4]</sup> However, the application of Raman spectroscopy in the analysis of organic dyes is limited because the high fluorescence emitted by the organic materials can mask the Raman emission preventing the analysis of these compounds. The use of surface-enhanced Raman scattering (SERS) can overcome this problem due to the huge intensification of the Raman emission and the fluorescence quenching that occurs on metal nanostructures, mediated by the plasmon resonance of selected metals such as Au and Ag.<sup>[5]</sup> SERS has been used as a micro-destructive technique for the characterization of organic dyes in works of art.<sup>[2,6]</sup> Among the different classes of colorants that can be analyzed by SERS, acidic dyes typically require much of an effort to be investigated, as they get electrostatically repulsed by the net negative charge of the nanoparticles interphase, which prevents the interaction analyte-substrate.

Acid Orange 20 (AO20, CI 14600), also called Orange I, is an acidic monoazo dye commercially available in the form of powdered Na<sup>+</sup> salt with a brown-red color.<sup>[1]</sup> Instead, when solubilized in water, it assumes a vivid orange hue. It is slightly soluble in ethanol and acetone and insoluble in most organic solvents.<sup>[8]</sup> The structure of AO20 consists of a naphthol unit and a sulfanated benzene ring linked together by an azo chromophore group (Figure 1). Phenylazonaphthols derivatives undergo an azo-hydrazone tautomerism that would arise from the removal of the hydroxyl hydrogen and the addition of this to the azo linkage with the consequent formation of keto (C=O), amino (N-H), and imino (C=N) groups in the keto tautomer. This behavior is common when the OH group is in *ortho* or *para* position in respect to the azo group. Different and several factors are accounted for the predominance of a tautomer over the other; despite the discrepancies, the literature suggests a majority of the hydrazone tautomer in acidic and neutral environment, while a (deprotonated) naphthol in the azo form should prevail at relatively strong basic pH.<sup>[9–11]</sup>

AO20 was one of the first soluble dyes to be commercialized, and was a popular food colorant in the

past,<sup>[13]</sup> until it was outlawed in 1956 (in the United States), after several cases reported sickness in children who ate candies colored with this dye.<sup>[14]</sup> Apart from food industries, Orange I also found application in textile manufacture (wool, silk), even if to a lesser extent respect to the closely related AO7, or Orange II, which carries the OH function in position 2 rather than

4. Also, it is employed as a dye for leather and as an indicator.<sup>[15]</sup>

In the present work, AO20, which lacks a comprehensive analytical study by Raman spectroscopy, in particular, from a cultural heritage point of view, was studied by means of UV-Vis, Raman, and SERS spectroscopies. In particular, given the structural nature of phenylazonaphthols, which undergo an acid-base tautomeric equilibrium, the Raman and SERS analyses of the solutions were performed at different pH conditions, in order to evaluate the preponderance of one tautomer over the other as a function of the pH. Theoretical density functional theory (DFT) calculations of the two tautomers were also performed and used for the spectra interpretation. Finally, the effect of pH on the morphology of metal nanoparticles employed as SERS substrates was evaluated.

## 2 | MATERIALS AND METHODS

### 2.1 | Reagents

AgNO<sub>3</sub>, hydroxylamine, trisodium citrate dihydrate, and sodium hydroxide were purchased from Sigma-Aldrich. Nitric acid was purchased from Merck. All aqueous solutions used for the silver colloid synthesis were prepared using MilliQ water.

For the UV-Vis and Raman analyses, stock solutions of the dye were prepared at a concentration of 10<sup>−2</sup> M. Solutions at different pH values were obtained by the addition of suitable microvolumes of diluted nitric acid or sodium hydroxide.

For the SERS analysis, AO20 10<sup>−4</sup> M aqueous solutions were prepared. Then, an aliquot of 100 μl was taken and added to 900 μl of the nanostars colloid, reaching a concentration of 10<sup>−5</sup> M.

### 2.2 | Preparation of Ag nanostars

The nanostars colloid was prepared following the procedure reported by Garcia-Leis *et al.*<sup>[16]</sup> Such SERS substrate is prepared by a two-step reduction process of AgNO<sub>3</sub>, first with neutral hydroxylamine, followed by another one with trisodium citrate dihydrate.

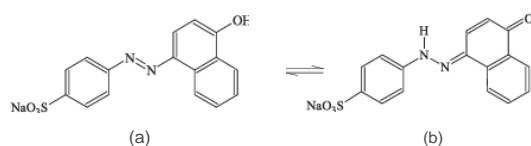


**FIGURE 1** Molecular structure of the AO20 (a) HA and (b) KH tautomers

## 2.3 Instrumentation

The UV/VIS/NIR absorbance spectra of the dyes solutions and of the colloidal dispersion were obtained with a Shimadzu 3600 UV/VIS/NIR spectrometer equipped with  $^2\text{H}$  and W lamps as sources and a photomultiplier (UV/VIS), a InGaAs and a PbS (NIR) as detectors. The baseline reference sample was prepared with 3 ml of MilliQ water.

Raman and SERS spectra at 442 and 532 nm were collected with a Renishaw inVia Raman Spectrometer, equipped with a Leica microscope, and an electrically refrigerated CCD camera. An He:Cd and a Nd:YAG laser were used as the 442 and 532 nm excitation lines, respectively. Measurements were taken using a Rayleigh line filter and different gratings were coupled with the different laser sources: 1800 L/mm at 532 nm and 2400 L/mm at 442 nm. Spectra were collected in the range 2000–100  $\text{cm}^{-1}$ . The maximum power at the samples when exciting with the 442 and 532 nm lines were 3 and 5 mW, respectively. Spectra were registered with an integration time of 10 s.

Raman and SERS spectra at 633 and 785 nm were collected with a Renishaw RM2000 Raman Microscope System equipped with a Leica microscope and an electrically refrigerated charge-coupled device camera (CCD). An He-Ne and a diode laser were used as the 633 and 785 nm excitation lines, respectively. Spectra were collected in the range 2800–100  $\text{cm}^{-1}$ . The maximum power at the samples with excitation at 633 and 785 nm were 2.5 and 2 mW, respectively. Spectra were registered with an integration time of 10 s.

Transmission electron microscopy (TEM) images were obtained using a JEOL JEM-2100 TEM operated at 200 kV, with a LaB6 filament. Digital images were recorded using an Orius Gatan CCD camera. The analyzed samples were prepared adding 100  $\mu\text{l}$  of  $10^{-4}$  M AO20 solution to 900  $\mu\text{l}$  of colloid, for an overall dye concentration of  $10^{-5}$  M. The samples were deposited on carbon coated grids and analyzed upon drying.

## 2.4 DFT calculations

For the hydro (HA) and keto (KH) AO20 tautomers, optimization of the ground state neutral singlet structures and calculation of the theoretical Raman spectra were performed with DFT using the Gaussian 09 package,<sup>11</sup> considering neutral sulfonate groups. All the calculations were performed in vacuum conditions, using a B3LYP hybrid exchange correlation functional in combination with 6-31G\*\* as a basis set. Upon optimization of the molecular geometry, Raman spectra were obtained. No

imaginary wavenumbers were observed in the calculated spectra. GaussView 5.09 was employed to view data and output images. Detailed assignments of the vibrational normal modes were based on the best fit comparison of the wavenumbers of calculated and experimental Raman bands. A scaling factor of 0.927 was employed in this work, as these factors are commonly used in the calculated spectra in order to correct the correlation effects that are only partially accounted for in DFT calculations.

## 3 RESULTS AND DISCUSSION

### 3.1 UV-Vis spectra of aqueous solutions at different pH

The effect of pH was studied first by UV-Vis absorption spectroscopy. The dye water solution ( $0.33 \times 10^{-4}$  M) showed a pH of  $\sim 4.7$ . Figure 2 (for the complete graph see figure S2) show that for pH 4.7, AO20 exhibits a maximum at 475 nm attributed to the  $\pi \rightarrow \pi^*$  electronic transition of C=N (KH- Figure 1b), a second absorption close to 290 nm (due to the  $\pi \rightarrow \pi^*$  of the naphthalene moiety), and a third one at around 335 nm (ascribable to the  $\pi \rightarrow \pi^*$  of the naphthalene with partly lost aromaticity because of KH formation).<sup>9</sup> Instead, for pH > 4.7 the last absorption completely disappears, while the band around 290–300 nm increases with pH. Most importantly, the maximum at 475 nm shifts to 515 nm, attributed to the  $\text{N}=\text{N} \pi \rightarrow \pi^*$  electronic transition of the HA tautomer (Figure 1a).<sup>9</sup> For pH higher than 4.7, the maximum not only shifts to higher wavelength, but also appears broader, going from a fwhm of 100 to 130 nm. In particular, it is possible to identify the presence of a slight

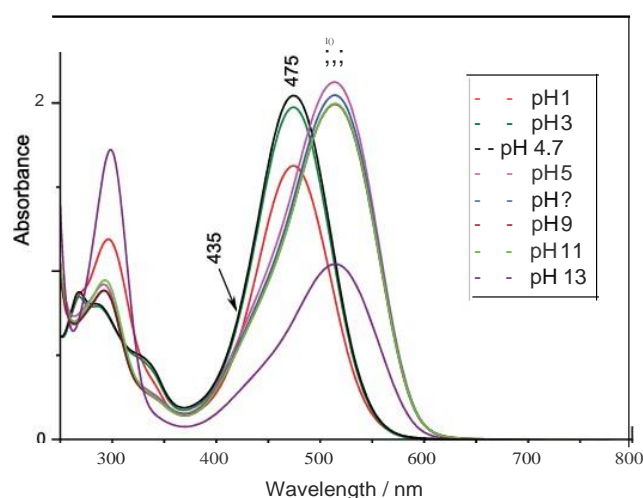


**FIGURE 2** UV-Vis spectra of  $0.33 \times 10^{-4}$  M AO20 aqueous solutions at different pH values [Colour figure can be viewed at [wileyonlinelibrary.com](http://wileyonlinelibrary.com)]

**FIGURE 4** Raman DFFcalculated spectra of the (a) KH and (e) HA tautomers of AO20. Raman spectra of 1.0<sup>-2</sup> M dye solutions at (b) pH < 4.7, (c) pH = 4.7, and (d) pH > 4.7. Excitation at 633 nm [Colour figure can be viewed at [wileyonlinelibrary.com](http://wileyonlinelibrary.com)]

**TABLE 1** Main experimental and calculated Raman wavenumbers ( $\text{cm}^{-1}$ ) of AO20 aqueous solutions at different pH and assignments derived from the DFT calculations (B3LYP6-31G\*\*)

$\nu_{\text{exp}} (\text{cm}^{-1})$ AO20 acidic	$\nu_{\text{exp}} (\text{cm}^{-1})$ AO20 pH 4.7	$\nu_{\text{exp}} (\text{cm}^{-1})$ AO20 alkaline	$\nu_{\text{cal.}} (\text{cm}^{-1})$ scaled	AO20 tautomer	Assignments
1620s	1620s		1649	KH	$\nu(\text{C}=\text{O})$ , $\nu(\text{C}=\text{C})\text{conj alkene}$ , $\nu(\text{C}=\text{N})$ , $\nu(\text{CC})\text{naph}$
		1590 <i>s</i>	1582	HA	$\nu(\text{CC})\text{naph}$ , $\nu(\text{N}=\text{N})$ , $\delta(\text{CH})$
1599 <i>vs</i>	1600 <i>vs</i>		1580	KH	$\nu(\text{CC})$ , $\delta(\text{NH})$ , $\nu(\text{C}=\text{C})\text{conj alk}$
		1574 <i>sh</i>	1564	HA	$\nu(\text{CC})\text{naph}$ , $\nu(\text{N}=\text{N})$ , $\delta(\text{CH})$
1553 <i>w</i>	1553 <i>w</i>		1543	KH	$\nu(\text{CC})\text{napht}$ , $\nu(\text{C}=\text{C})\text{conj alk}$ , $\delta(\text{CH})$ , $\delta(\text{NH})$
		1536 <i>vw</i>	1546	HA	$\nu(\text{CC})\text{benz}$ , $\delta(\text{CH})\text{benz}$
1504 <i>m</i>	1504 <i>m</i>		1502	HA	$\nu(\text{CC})\text{napht}$
1480m	1479 <i>m</i>	1486 <i>vw</i>	1470	KH	$\nu(\text{CC})\text{benz}$ , $\delta(\text{CH})\text{benz}$ , $\nu(\text{Cbenz-N})$ , $\nu(\text{C}=\text{N})$
1452 <i>m</i>	1452m		1455	KH	$\nu(\text{CC})$ , $\delta(\text{CH})$ , $\delta(\text{NH})$ , $\nu(\text{C}=\text{N})$
1436 <i>sh</i>	1436 <i>sh</i>		1436	KH	$\nu(\text{CC})\text{napht}$ , $\nu(\text{C}=\text{N})$ , $\delta(\text{CH})\text{naph}$ , $\delta(\text{NH})$
1412 <i>w</i>	1414w	1419 <i>s</i>	1422	HA	$\nu(\text{N}=\text{N})$ , $\nu(\text{CC})\text{napht}$ , $\delta(\text{CH})\text{napht}$
1376 <i>vw</i>			1386	KH	$\nu(\text{CC})\text{benz}$ , $\delta(\text{NH})$ , $\delta(\text{CH})\text{benz}$
		1376 <i>s</i>	1377	HA	$\nu(\text{CC})\text{naph}$ , $\delta(\text{CH})\text{naph}$
		1359 <i>s</i>	1359	HA	$\nu(\text{CC})\text{napht}$ , $\delta(\text{O H})$ , $\delta(\text{CH})\text{napht}$
1348 <i>vw</i>	1348 <i>vw</i>	1345 <i>sh</i>	1344	HA	$\nu(\text{CC})\text{napht}$ , $\delta(\text{O H})$ , $\nu(\text{N}=\text{N})$ , $\delta(\text{CH})\text{napht}$
1320m	1319 <i>m</i>		1330	KH	$\nu(\text{CC})$ , $\delta(\text{NH})$ , $\delta(\text{Cnaph NN})$
		1320 <i>m</i>	1315a	HA	$\nu(\text{CC})\text{benz}$ , $\delta(\text{C-S})$
1305 <i>m</i>	1305 <i>m</i>	1303 <i>m</i>	1297	KH	$\nu(\text{CC})$ , $\nu(\text{S-O})$
1283 <i>m</i>		1280 <i>m</i>	1278	KH	$\nu(\text{CC})\text{benz}$
1267 <i>sh</i>	1263 <i>w</i>		1268	KH	$\nu(\text{NN})$ , $\delta(\text{CH})$ , $\nu(\text{CC})\text{naph}$
		1263 <i>sh</i>	1262	HA	$\delta(\text{CH})$ , $\nu(\text{NN})$
1239 <i>w</i>	1236 <i>vw</i>	1227 <i>w</i>	1242	HA	$\delta(\text{CH})\text{napht}$ , $\nu(\text{C-N})$ , $\nu(\text{CC})\text{napht}$
1211 <i>w</i>	1211 <i>w</i>		1210	KH	$\delta(\text{CH})\text{napht}$ , $\nu(\text{Cbenz-N})$
		1195 <i>s</i>	1180	HA	$\delta(\text{Cnaph-N})$ , $\delta(\text{Cbenz-N})$ , $\delta(\text{CH})$ , $\delta(\text{OH})$
1177 <i>m</i>	1177 <i>m</i>		1173	KH	$\nu(\text{breath})\text{benz}$ , $\nu(\text{S-O})$ , $\delta(\text{CH})\text{benz}$
1164 <i>sh</i>	1164 <i>sh</i>	1167 <i>s</i>	1164	HA	$\delta(\text{OH})$ , $\nu(\text{C-O})$ , $\delta(\text{CH})\text{naph}$
		1143 <i>s</i>	1144	HA	$\delta(\text{CH})$
1123 <i>w</i>	1123 <i>w</i>	1118vs	1120	HA	$\delta(\text{CH})$
		1073 <i>vw</i>	1069	HA	$\nu(\text{as breath})\text{benz}$ , $\nu(\text{C-S})$
1059 <i>w</i>			1072	KH	$\nu(\text{as breath})\text{benz}$ , $\nu(\text{C-S})$
		1030 <i>m</i>	1037	HA	$\delta(\text{CCC})\text{naph}$ , $\nu(\text{C-O})$
1021 <i>vw</i>	1021 <i>vw</i>	1021 <i>w</i>	1018	HA	$\nu(\text{breath})\text{naph}$
1005 <i>w</i>	1005 <i>w</i>		1004	KH	$\nu(\text{breath})\text{naph}$
		1002 <i>vw</i>	992	HA	$\nu(\text{breath})\text{naph}$ , $\delta(\text{CCC})\text{benz}$
950 <i>vw</i>	950 <i>vw</i>		950	KH	$\nu(\text{breath})\text{benz}$ , $\nu(\text{S-O})$
892 <i>w</i>	892 <i>vw</i>	917w	895	HA	$\delta(\text{CNNC})$ , $\delta(\text{CCC})$

(Continues)



**TABLE 1** (Continued)

$\nu_{\text{exp}} (\text{cm}^{-1})^a$ AO20 acidic	$\nu_{\text{exp}} (\text{cm}^{-1})^a$ AO20 pH 4.7	$\nu_{\text{exp}} (\text{cm}^{-1})^a$ AO20 alkaline	$\nu_{\text{calc}} (\text{cm}^{-1})$ scaled	AO20 tautomer	Assignments <sup>b</sup>
		730w	708	HA	5 (CCC)
705 <i>vw</i>	705vw		708	KH	5 (CCC)
638 <i>w</i>	638vw	638 <i>vw</i>	669	HA	5 (CCC)
568 <i>w</i>	568w	569w	547	KH, HA	5 (CCC)
520w	520w	520w	500	HA	5 (CCC)
474vw	474vw	480w	476	KH	y (CCC)
443 <i>m</i>	443 <i>m</i>		422	KH	5 (CCC)
355 <i>vw</i>	355 <i>vw</i>		327	KH	5 (CCC)

<sup>a</sup>*vw*, very weak; *w*, weak; *m*, medium; *s*, strong; *vs*, very strong; *sh*, shoulder.

<sup>b</sup>*h*<sub>v</sub>, stretching; 5, in-plane bending; *y*, out-of-plane bending; *s*, symmetric; *as*, antisymmetric.

The Raman spectra of at pH 3; 4.7 are similar, as no significant changes are observed, except from a band at around 1080  $\text{cm}^{-1}$  and the broadening of bands in the region of 1370  $\text{cm}^{-1}$  for pH below 4.7. The main bands of the Raman spectra were listed above. However, at pH > 4.7, the Raman spectrum is completely different from the other ones. At these pH values, the main Raman bands are observed at 1592, 1419, 1376, 1359, 1320, 1303, 1280, 1263, 1195, 1162, 1143, 1118, 1030, 917, 812, 730, 569 and 480  $\text{cm}^{-1}$ . From the UV-Vis spectroscopic study of AO20, it can be deduced that this Raman spectrum is due to the HA tautomer of the dye.

The DFT calculated Raman spectra of the KH and HA tautomer show a very good fit with the experimental Raman spectra of the keto and hydro geometries (Figure S1), not only in the wavenumbers but also in the intensity of the bands. This indicates the suitability of the level of theory used and an appropriate selection of basis set for the AO20 tautomers. The assignments of vibrational normal modes derived from the calculations are shown in Table 1. From the bands assignment, it is possible to confirm that AO20 is found prevalently as the KH tautomer for pH 3; 4.7, while the azo form is found for higher pH values. Thus, at pH 3; 4.7, the characteristic Raman bands of the KH tautomer can be identified. The band at 1620  $\text{cm}^{-1}$  is associated to the stretching of the C=O bond conjugated with the C=C (and possibly with the C=N) of KH. The most intense band of the Raman spectrum is observed at 1600  $\text{cm}^{-1}$  and is assigned to the deformation of the NH and the stretching of the C=C conjugated group. The band at 1504  $\text{cm}^{-1}$  is due to the  $\nu(\text{C}=\text{N})$  while the bands at 1452 and 1436  $\text{cm}^{-1}$  are attributed to both 6 (NH) and  $\nu(\text{N}=\text{N})$ , only present in the KH tautomer. Other bands assigned to 6 (NH) are those at 1553, 1379, and 1319  $\text{cm}^{-1}$ . The medium intensity band at 1177  $\text{cm}^{-1}$  is associated to the breathing and CH deformation modes of the benzene ring and to the

stretching of S-O. For pH higher than 4.7, these bands are missing or weak. However, significant bands are observed as those at 1590 and 1419  $\text{cm}^{-1}$ , assigned to  $\nu(\text{N}=\text{N})$  only present in the HA tautomer. Other minor bands associated with the azo group are located at 1574 and 1345  $\text{cm}^{-1}$ . Besides, in the region 1100- 1200  $\text{cm}^{-1}$  four intense bands, at 1195, 1167, 1143, and 1118  $\text{cm}^{-1}$ , can be attributed to the symmetric stretching and deformation of 6 (C-N), 6 (OH),  $\nu(\text{C}-\text{O})$ , and 6 (CH). Moreover, another intense band at 1359  $\text{cm}^{-1}$  is observed, assigned to 6 (OH) of the HA tautomer. Finally, the medium intensity band at 1030  $\text{cm}^{-1}$  is associated to  $\nu(\text{C}-\text{O})$ . According to the review by Trotter *et al.*<sup>120</sup> in phenylazonaphthols, the vibrational modes  $\nu(\text{N}=\text{N})$ , 6 (C-N), and  $\nu(\text{C}-\text{N})$  are observed between 1380- 1450, 1160- 1200, and 1130- 1160  $\text{cm}^{-1}$ , respectively, supporting our interpretation.

### 3.4 SERS spectra at different pH

SERS spectra of AO20 were obtained at different pH values: 5- 5.3, which is the pH of the dye solution on the Ag NST suspension; and 3, after the addition of  $\text{HNO}_3$ . As it was demonstrated above, at the former pH, AO20 is predominantly present as the HA tautomer, while at the latter, as the KH.

The SERS spectra were gathered using 442, 532 and 633 nm excitation lines and are shown in Figures SI, SII and SIII, respectively. It is easy to observe that in all cases the SERS spectra at pH 3, where in solution the KH tautomer is dominant, was always the most intense. No significant differences are shown among these spectra. The main SERS bands are observed at 1615, 1597, 1545, 1501, 1449, 1356, 1302, 1253, 1178, 1147, 1122, 996, 949, 892, 723, 630, 571, 559, 455, 401 and 367  $\text{cm}^{-1}$ . The high intensity of the SERS spectra at pH < 4.7 is due to the



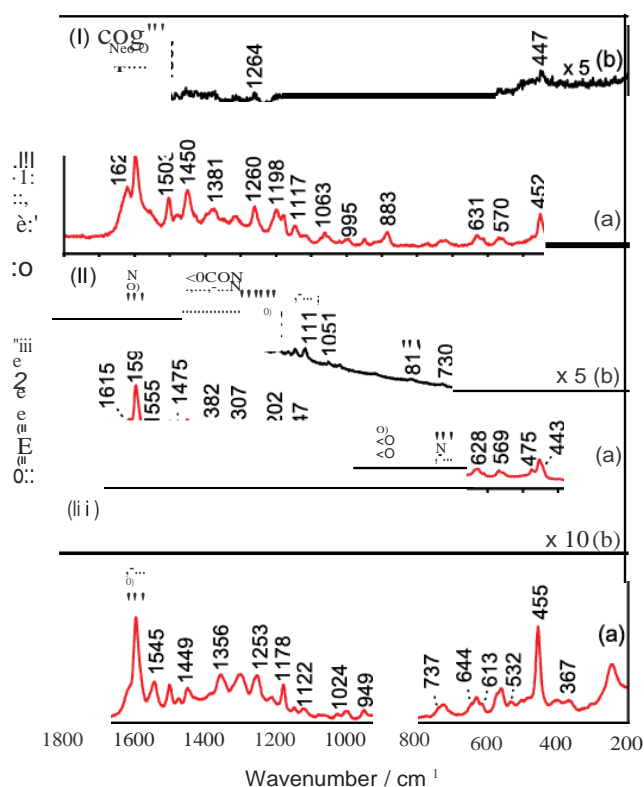


**FIGURE 5** SERS spectra of  $1.0 \times 10^{-5}$  M AO20 at (I) 442, (II) 532 and (III) 633 nm excitation lines and pH (a) 3 and (b)  $\sim 5.3$  [Colour figure can be viewed at [wileyonlinelibrary.com](http://wileyonlinelibrary.com)]

protonation of the sulfonic group of AO20. This makes the molecule to reduce its negative charge and become neutral, lowering the electrostatic repulsion between the dye and the negatively charged Ag NST. This fact leads to the increase of the AO20-Ag interaction strength.

Great differences can be observed in the SERS spectra at pH 5.3 obtained at the different excitation lines. At 442 nm the SERS spectrum at pH  $> 4.7$  (Figure 5Ib) several bands, such as those at 1626, 1600, 1505, 1264, 1182, 496, and  $477 \text{ cm}^{-1}$ , are observed, although their intensity is quite low. These are the same SERS bands appearing at lower pH (Figure 5Ia). Therefore, at this excitation wavelength, only the KH tautomer is detected, regardless of the pH of the media. This can be due to the resonant conditions that occur at 442 nm, as previously observed in the Raman spectrum of the AO20 aqueous solution. In this case, as the pH is close to the  $pK_a$  of the dye, some molecules of the dye could still be present as the KH tautomer. Because the SERS bands of this tautomer are enhanced by resonance, only KH is detected at 442 nm, although its proportion at pH 5.3 is much lower. At 532 nm, the SERS spectrum at pH  $> 4.7$  (Figure 5IIb) shows bands at 1592, 1418, 1376, 1360, 1322, 1303, 1282, 1197, 1165, 1145, 1117, 1051 and  $1019 \text{ cm}^{-1}$ . These bands are similar to those observed in the Raman spectrum of the AO20 solution at alkaline pH. This means that the

HA tautomer is selectively detected at this excitation line. This is due to the preresonant Raman effect that occurs at 532 nm, as this wavelength is close to the absorption maximum of the HA tautomer at 515 nm, attributed to the  $1t-1t^*$  transition of the  $N=N$  chromophore.<sup>119</sup> The SERS spectrum of AO20 at pH 5.3 recorded at 633 nm does not show any band. As discussed above, the adsorption process is difficult at this pH value, and none of the tautomers is excited in resonance conditions.

### 3.5 | Comparison of the Raman and SERS spectra: Adsorption mechanism

By comparison of the Raman and SERS spectra of AO20 at pH  $< 4.7$  (Figures 4b and 5IIIa, respectively), the SERS spectrum obtained at 633 nm resembles more that of the KH tautomer. However, some changes in the relative intensities of the bands are observed. It can be observed that the band around  $1480 \text{ cm}^{-1}$ , assigned to  $||(\text{C}=\text{N})$  and  $||\text{C}=\text{N}$ , decreases in intensity in the SERS spectrum. However, several bands are enhanced in the SERS spectrum: the most enhanced one, at  $455 \text{ cm}^{-1}$ , is assigned to 5 (CCC). Other bands whose intensity is increased are those at 1545, 1449, 1356, 1253, 1147, 1024, 723, 630, 401, and  $367 \text{ cm}^{-1}$ . All these bands are attributed to in plane normal modes. This suggests a perpendicular interaction of the KH tautomer of AO20 with the Ag NST. Another interesting change is the shift of the Raman band at 1620 to  $1615 \text{ cm}^{-1}$ . This observation is related to the decrease of the double bond character of the normal modes involved in this vibration such as  $\text{C}=\text{O}$ ,  $\text{C}=\text{C}$  and  $\text{C}=\text{N}$ , due to the adsorption of the dye onto the Ag NST. Thus, a perpendicular interaction of AO20 through the  $\text{C}=\text{O}$  group is proposed on the Ag surface. This will produce a delocalization on the conjugated double bonds of the molecule. This type of interaction was previously observed in other aromatic molecules.<sup>121–23</sup> In the particular case of AO20, a charge-transfer process also occurs between the  $\text{C}=\text{O}$  group and the metal. This mechanism is further enhanced by the azo group in *para* position that also contributes to this electron transference and could contribute to the tautomerization as well.

The comparison of the Raman and SERS spectra of AO20 at pH  $> 4.7$  (Figures 4d and 5IIb, respectively) is more difficult than the previous one. This is due to the low intensity of the SERS bands observed in the spectrum at pH 5.3 obtained at 532 nm, the only one in which the HA tautomer is detected. There is not a clear enhancement of any band in the SERS spectrum. The greatest decrease in intensity is observed in the band at  $1118 \text{ cm}^{-1}$ , which is associated to 5 (CH). A slight

decrease of several Raman bands is observed, such as those at 1590, 1359, 1303, 1280 and 1030  $\text{cm}^{-1}$ . Most of these bands are attributed to in plane vibrations of the CC and CH groups. Thus, we could suggest a perpendicular orientation of the HA tautomer on the Ag surface. The interaction could take place through the OH or  $\text{SO}_3$  groups.

### 3.6 I TEM analysis of Ag NST at different pH

Figure 6 shows the TEM micrographs obtained from the Ag NST solution and Ag + dye dispersions, with and without pH modification. These images allow the characterization of the Ag NPs as branched particles with variable dimensions in the range of 50- 200 nm, that tend to aggregate in clusters of micrometric sizes. The presence

of a dye at pH 5.3 results as a blurred capping on top of the NST. Such effect suggests a low interaction between the Ag and the dye molecules, due to repulsion forces acting within the negatively charged interphase of the Ag NPs and the AO20 molecule, that should be deprotonated. Besides, the presence of the dye seems to cause an aggregation of the colloid. It is interesting to note that at pH 4 such blurred capping is no longer present. This could be explained by affinity of the neutral AO20 molecule and the Ag NST. Indeed, the effect of diminishing the pH does not only reduce the electrostatic repulsions, but also increases the nanoparticles surface availability on behalf of the dye by partially protonating the carboxylic functions of citrate molecules, which are released from the Ag NPs surface. However, the acidic pH modifies the morphology of the Ag NST colloid that appears characterized by a lesser extent on NPs branches. Again, such effect can be recalled to the instability of

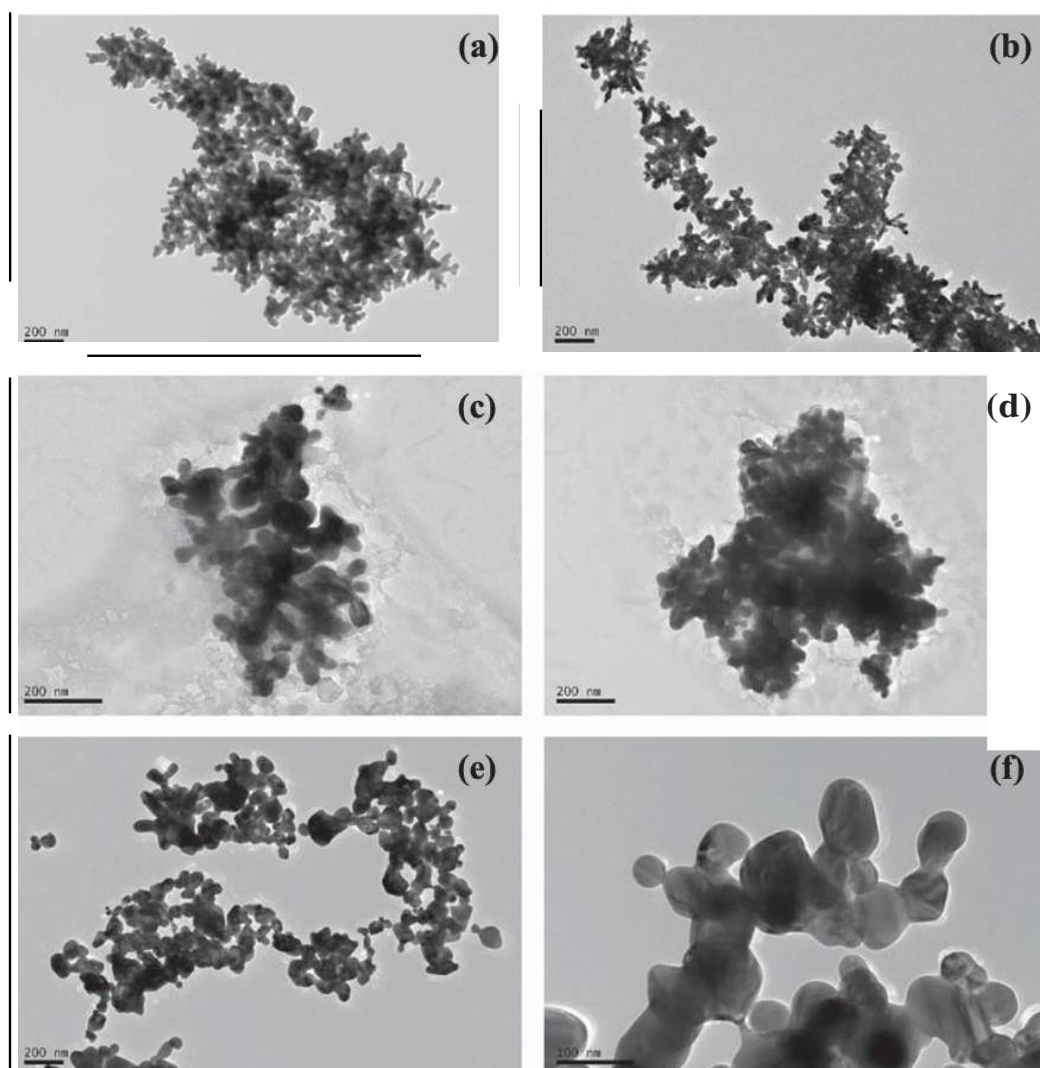


**FIGURE 6** TEM micrographs of (a, b) Ag NST and Ag NST + AO20 solution at (c, d) pH  $\sim$  5.3 and (e, f) pH 4

hydroxylamine in acidic environment.<sup>31</sup> For this reason, the general improvement in signal quality observed in SERS spectra of AO20 at acidic pH, rather than being attributed to the great enhancement of the LSPR at the vertices and interstices of the NST, should be accounted to a most effective adsorption of the dye on the Ag NPs.

negatively charged interphase of the Ag NPs and the AO20 ion.

## 4 | CONCLUSIONS

In this work, the monoazo dye Acid Orange 20 which dye undergoes an azo-hydrazone tautomerism was analyzed by UV-Vis, Raman, and SERS spectroscopies. For this reason, these spectroscopic techniques were applied in order to evaluate the preponderance of one tautomer over the other in different pH conditions. The UV-Vis spectra showed that at pH 4.7, the dye was present as the KH tautomer, while at higher pH values, HA was prevalent. Raman spectra of solid and aqueous solutions of AO20 at different excitation wavelengths showed bands at 1620, 1600, 1504, 1479, 1452, 1319, 1305, 1177, 1005, 568, 520 and 443  $\text{cm}^{-1}$ . As the pH of the solutions was 4.7, these Raman bands were assigned to the KH tautomer. The Raman spectra of AO20 solutions at pH above 4.7 showed bands at 1592, 1419, 1376, 1359, 1320, 1303, 1280, 1263, 1195, 1162, 1143, 1118, 1030, 917, 812, 730, 569 and 480  $\text{cm}^{-1}$ , and was assigned to the HA tautomer. The Raman spectra at pH 4.7 corresponded to KH. Vibrations obtained by DFT calculations of the tautomers were successfully assigned to the experimental Raman bands of HA and KH. Thus, bands of the N=N, OH, C=O, and C-N groups were assigned to bands of HA, and N-N, C=O, C=C, and N-H to bands of KH. In the SERS spectrum of AO20 at 442 nm only KH was detected, even at pH > 4.7 due to preresonance conditions of this tautomer at that excitation line. However, in the SERS spectrum at 532 nm and pH 5, the HA tautomer could be detected due to resonance conditions at that wavelength. At 633 nm, none of the tautomers were detected in the SERS spectrum at pH > 4.7 due to lack of resonance of HA and KH. According to these results, the best experimental conditions for the analysis of AO20 in works of art are the use of an acidic pH, below 4, and an excitation line close to 532 nm. Thus, the obtained SERS spectra will benefit from the strong interaction of the dye with the Ag nanoparticles and the preresonance effect that increases the enhancement. From the comparison of the Raman and SERS spectra of the dye, a perpendicular orientation of AO20 was proposed as the adsorption geometry of the dye with the metallic substrate. The TEM images of the Ag NST show a blurred capping on the NPs at pH 5.3, which suggests a low interaction dye-Ag. This is attributed to repulsion forces acting within the

